ELSEVIER

Comput. Methods Appl. Mech. Engrg. 181 (2000) 393–401

Computer methods in applied mechanics and engineering

www.elsevier.com/locate/cma

Numerical simulation of the smooth quantum hydrodynamic model for semiconductor devices

Carl L. Gardner [*,1], Christian Ringhofer [2]

Department of Mathematics, Arizona State University, Tempe, AZ 85287-1804, USA

Received 1 May 1998

Abstract

An extension of the classical hydrodynamic model for semiconductor devices to include quantum transport effects is reviewed. This "smooth" quantum hydrodynamic (QHD) model is derived specifically to handle in a mathematically rigorous way the discontinuities in the classical potential energy which occur at heterojunction barriers in quantum semiconductor devices. A conservative upwind discretization of the one-dimensional (1D) steady-state smooth QHD equations is outlined. Smooth QHD model simulations of the resonant tunneling diode are presented which exhibit enhanced negative differential resistance when compared with simulations using the original $O(\hbar^2)$ QHD model. © 2000 Elsevier Science S.A. All rights reserved.

Keywords: Quantum hydrodynamic model; Semiconductor devices; Numerical simulations; Electron tunneling

1. Introduction

Quantum transport effects including electron or hole tunneling through potential barriers and buildup in quantum wells are important in predicting the performance of ultra-small semiconductor devices. These effects can be incorporated into the hydrodynamic description of charge propagation in the semiconductor device.

Refs [1,2] present an extension of the classical hydrodynamic model to include quantum transport effects. This "smooth" quantum hydrodynamic (QHD) model is derived specifically to handle in a mathematically rigorous way the discontinuities in the classical potential energy which occur at heterojunction barriers in quantum semiconductor devices. The model is valid to all orders of $\hbar^2/(mTl^2)$ (where m is the effective mass of electrons or holes, T the temperature, and l is a typical length scale for the problem) and to first order in the classical potential energy.

The smooth QHD equations have the same form as the classical hydrodynamic equations (for simplicity we consider just electron flow):

$$\frac{\partial n}{\partial t} + \frac{\partial}{\partial x_i}(nu_i) = 0, \tag{1}$$

* Corresponding author. Tel.: +1-602-965-0226; fax: +1-602-965-0461.
E-mail address: gardner@math.la.asu.edu (C.L. Gardner).

[1] Research supported in part by the US Army Research Office under grant DAAH04-95-1-0122 and by the National Science Foundation under grants DMS-9706792 and INT-9603253.

[2] Research supported in part by the National Science Foundation under grants DMS-9706792 and INT-9603253.

PII: S0045-7825(99)00180-2

$$\frac{\partial}{\partial t}(mnu_j) + \frac{\partial}{\partial x_i}(mnu_i u_j - P_{ij}) = -n\frac{\partial V}{\partial x_j} - \frac{mnu_j}{\tau_p}, \tag{2}$$

$$\frac{\partial W}{\partial t} + \frac{\partial}{\partial x_i}(u_i W - u_j P_{ij} + q_i) = -nu_i\frac{\partial V}{\partial x_i} - \frac{\left(W - \frac{3}{2}nT_0\right)}{\tau_w}, \tag{3}$$

where n is the electron density, u_i is the velocity, m is the effective electron mass, P_{ij} is the stress tensor, V is the potential energy, W is the energy density, q_i is the heat flux, and T_0 is the temperature of the semiconductor lattice (k_B is set equal to 1). Indices i, j equal 1, 2, 3, and repeated indices are summed over. Electron scattering is modeled by the standard relaxation time approximation (see e.g., Ref. [3]), with momentum and energy relaxation times τ_p and τ_w.

The stress tensor and energy density are:

$$P_{ij} = -nT\delta_{ij} - \frac{\hbar^2 n}{4mT}\frac{\partial^2 \overline{V}}{\partial x_i \partial x_j}, \tag{4}$$

$$W = \frac{3}{2}nT + \frac{1}{2}mnu^2 + \frac{\hbar^2 n}{8mT}\nabla^2 \overline{V}, \tag{5}$$

where T is the temperature of the electron gas and the "quantum" potential $\overline{V}$ is given by ($\beta = 1/T$):

$$\begin{aligned}\overline{V}(\beta, \mathbf{x}) = & \int_0^\beta \frac{\mathrm{d}\beta'}{\beta}\left(\frac{\beta'}{\beta}\right)^2 \int \mathrm{d}^3x' \left(\frac{2m\beta}{\pi(\beta-\beta')(\beta+\beta')\hbar^2}\right)^{3/2} \\ & \times \exp\left\{-\frac{2m\beta}{(\beta-\beta')(\beta+\beta')\hbar^2}(\mathbf{x}'-\mathbf{x})^2\right\} V(\mathbf{x}').\end{aligned} \tag{6}$$

The transport Eqs. (1)–(3) are coupled to Poisson's equation for the electrostatic potential energy

$$\nabla \cdot (\epsilon \nabla V_P) = e^2(N - n), \tag{7}$$

where ϵ is the dielectric constant, $e > 0$ is the electronic charge, and N is the density of donors. The total potential energy V consists of two parts, one from Poisson's equation V_P and the other from the potential barriers V_B:

$$V = V_B + V_P. \tag{8}$$

V_B has a step function discontinuity at potential barriers.

To leading order in βV we have the equivalent "exponential" form of the smooth QHD model:

$$P_{ii} \approx -nT \ \exp\left\{\frac{\hbar^2}{4mT^2}\frac{\partial^2 \overline{V}}{\partial x_i^2}\right\} \quad \text{(no sum)}, \tag{9}$$

$$W \approx \frac{1}{2}mnu^2 + \frac{3}{2}nT \ \exp\left\{\frac{\hbar^2}{12mT^2}\nabla^2 \overline{V}\right\}. \tag{10}$$

This form guarantees that the pressure and energy density are always positive.

To derive the stress tensor and energy density, we construct an effective density matrix as an $O(\beta V)$ solution to the Bloch equation. Then using the momentum-shifted effective density matrix, we take moments of the quantum Liouville equation to derive the smooth QHD equations [1].

The original $O(\hbar^2/(mTl^2))$ QHD equations (see Refs. [4,5] and references therein) have been remarkably successful in simulating the effects of electron tunneling through potential barriers including single and multiple regions of negative differential resistance and hysteresis in the current–voltage curves of resonant tunneling diodes [5–7]. The stress tensor and energy density for the $O(\hbar^2/(mTl^2))$ model are the same as in Eqs. (4) and (5), with $\overline{V}$ replaced by its $\hbar^2/(mTl^2) \to 0$ approximation

$$\overline{V} = \frac{V}{3} + O(\hbar^2/(mTl^2)). \tag{11}$$

However, in order to avoid infinite derivatives at heterojunctions, the model relies on replacing (third) derivatives of the potential with derivatives of the logarithm of the electron density using the thermal equilibrium ansatz

$$n \sim \exp\{-\beta V\}. \tag{12}$$

The thermal equilibrium ansatz breaks down for applied voltages ΔV for which $\beta\Delta V \sim 1$.

The smooth QHD transport equations have four hyperbolic modes and one parabolic heat conduction mode. The original $O(\hbar^2/(mTl^2))$ QHD transport equations in contrast have two hyperbolic modes, two Schrödinger modes, and one parabolic mode. The dispersive Schrödinger modes are mathematically problematic [8] for transonic flows in which the electron velocity v changes from supersonic ($v > c$) to subsonic ($v < c$), where $c = \sqrt{T/m}$ is the sound speed in the electron gas. (For further analysis of transonic flow in a semiconductor device, see Ref. [9]).

2. Derivation of the smooth QHD model

One major difference between classical and quantum kinetic theory is that in quantum kinetic theory there is a separate equation that governs thermal equilibrium. In the quantum regime the classical Maxwellian distribution function is replaced by the equilibrium Wigner distribution function $f_W(\mathbf{x}, \mathbf{p})$. f_W is the Fourier transform of the density matrix corresponding to the operator $\exp(-\beta H)$, where H denotes the Hamiltonian operator. In thermal equilibrium, the density matrix $\rho(\mathbf{x}, \mathbf{y})$ satisfies the Bloch equation:

$$\frac{\partial \rho}{\partial \beta} = -\frac{1}{2}(H_x + H_y)\rho = \frac{\hbar^2}{4m}\left(\nabla_x^2 + \nabla_y^2\right)\rho - \frac{1}{2}[V(\mathbf{x}) + V(\mathbf{y})]\rho, \tag{13}$$

where $H_x = -\hbar^2\nabla_x^2/(2m) + V(\mathbf{x})$ and where we have assumed Boltzmann statistics. In Ref. [1], we solved the Bloch equation for the effective density matrix in the Born approximation using a Green's function method.

The effective density matrix has the form

$$\rho(\beta, \mathbf{x}, \mathbf{y}) \approx \left(\frac{m}{2\pi\beta\hbar^2}\right)^{3/2} \exp\left\{-\frac{m}{2\beta\hbar^2}(\mathbf{x} - \mathbf{y})^2 - \beta\tilde{V}(\beta, \mathbf{x}, \mathbf{y})\right\}, \tag{14}$$

where $\tilde{V}$ is given in center-of-mass coordinates $\mathbf{R} = \frac{1}{2}(\mathbf{x} + \mathbf{y})$, $\mathbf{s} = \mathbf{x} - \mathbf{y}$ by

$$\tilde{V}(\beta, \mathbf{R}, \mathbf{s}) = \frac{1}{2\beta}\int_0^\beta \mathrm{d}\beta' \int \mathrm{d}^3x' \left(\frac{2m\beta}{\pi(\beta - \beta')(\beta + \beta')\hbar^2}\right)^{3/2} \times \exp\left\{-\frac{2m\beta}{(\beta - \beta')(\beta + \beta')\hbar^2}x'^2\right\}\left[V\left(\mathbf{x}' + \mathbf{R} + \frac{\beta'}{2\beta}\mathbf{s}\right) + V\left(\mathbf{x}' + \mathbf{R} - \frac{\beta'}{2\beta}\mathbf{s}\right)\right]. \tag{15}$$

This quantum Maxwellian smooths out discontinuities in the classical potential, effectively lowering barrier heights, as well as extending their effects over a finite distance. The smooth quantum Maxwellian is contrasted with the (Fourier transform of the) classical Maxwellian in Figs. 1 and 2.

Dynamic evolution of the density matrix (including departures from thermal equilibrium) is governed in quantum kinetic theory by the quantum analog of the Boltzmann equation, the Wigner–Boltzmann or quantum Liouville equation:

$$i\hbar\frac{\partial \rho}{\partial t} + \frac{\hbar^2}{m}\nabla_R \cdot \nabla_s \rho = \left[V\left(\mathbf{R} + \frac{\mathbf{s}}{2}\right) - V\left(\mathbf{R} - \frac{\mathbf{s}}{2}\right)\right]\rho - i\hbar\left(\frac{1}{\tau}\mathbf{s} \cdot \nabla_s \rho + \frac{mT_0}{\hbar^2\tau}s^2\rho\right). \tag{16}$$

Scattering is modeled in Eq. (16) by Fokker–Planck terms (the last two terms on the right-hand side) in order to produce relaxation time scattering terms in the QHD conservation laws (2) and (3) for momentum and energy [10].

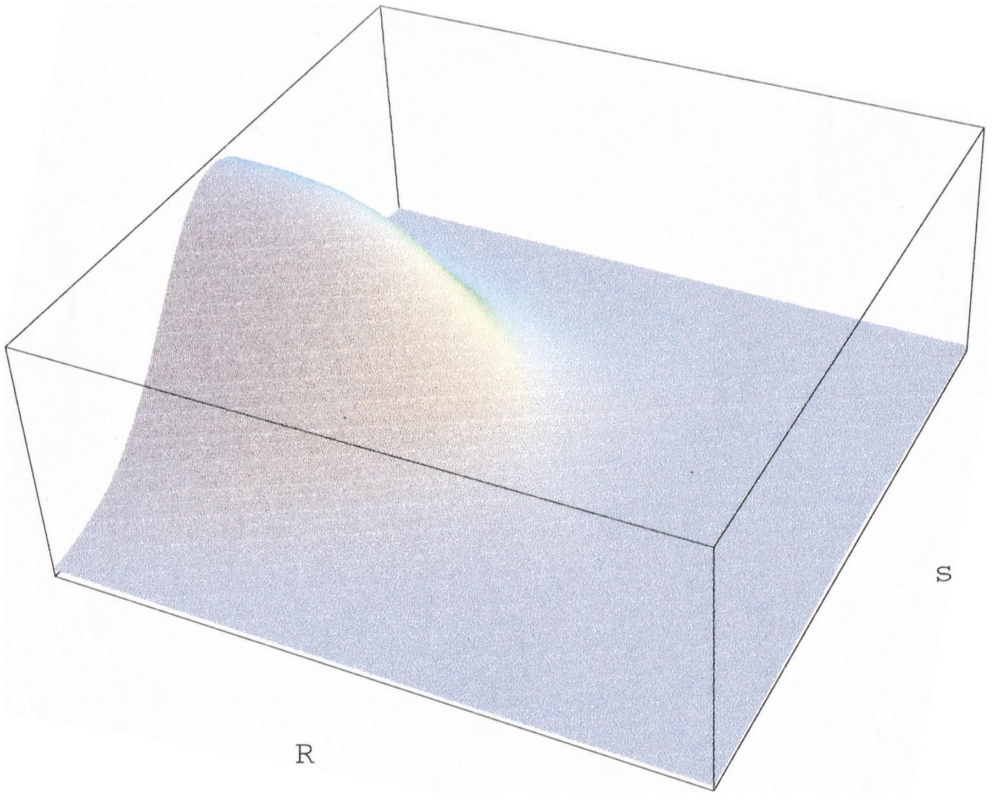

Fig. 1. Smooth quantum Maxwellian for a 0.1 eV potential step for electrons in GaAs at 300 K.

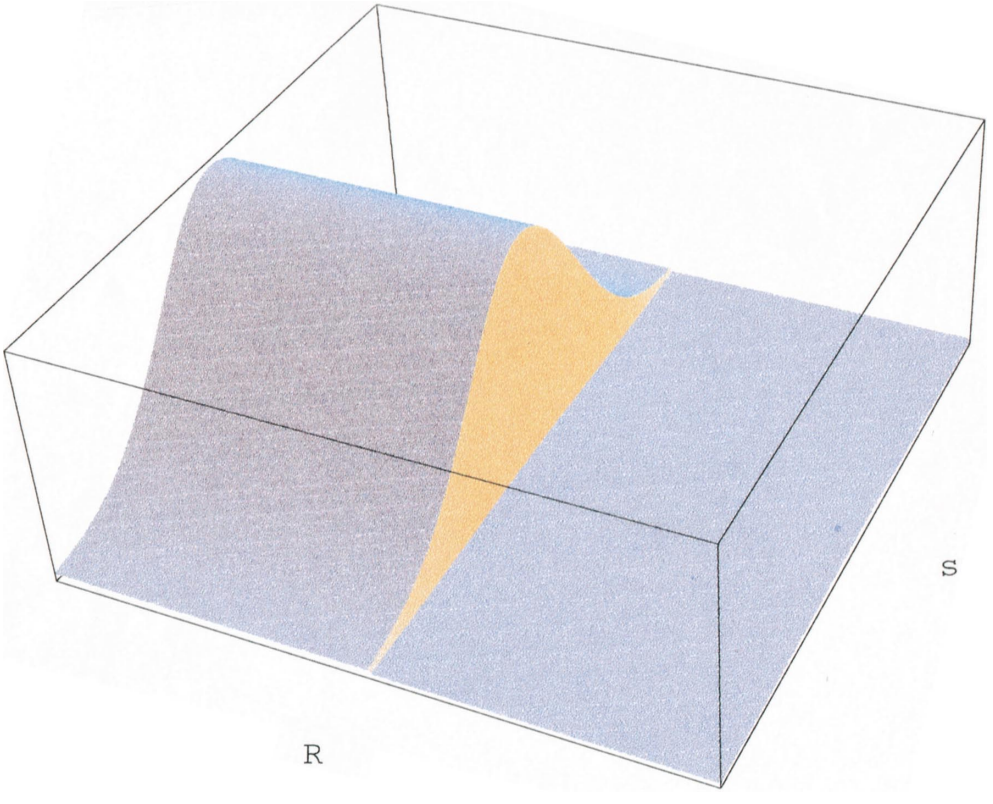

Fig. 2. Classical Maxwellian for a 0.1 eV potential step for electrons in GaAs at 300 K.

The moment expansion of the quantum Liouville equation is then obtained by multiplying the quantum Liouville equation with powers of $\hbar\nabla_s/i$ (1, $\hbar\nabla_s/i$, and $-\hbar^2\nabla_s^2/2m$, respectively) and taking the limit $\mathbf{s} \to 0$ to obtain conservation laws for electron number, momentum, and energy (see Ref. [1]).

The original QHD model can be derived via an $O(\hbar^2/(mTl^2))$ approximation of the solution of the Bloch equation (13), which yields the effective density matrix (14) with the smooth effective potential $\tilde{V}$ replaced by its limiting value $V/3$. For smooth potentials the smooth QHD model can be expected to agree closely with the original QHD model near the classical limit. However, taking moments of the quantum Liouville equation (i.e., differentiating the effective density matrix with respect to **s**) causes severe analytical problems in the case of discontinuous potentials. These problems are avoided in the smooth QHD model.

The smooth QHD equations avoid the second derivatives of a delta function that occur at heterojunction discontinuities in the $O(\hbar^2/(mTl^2))$ theory (before using the ansatz (12)). In fact, the smooth QHD equations contain at worst a step function discontinuity.

To see this, we define the 1D smooth effective potential in the momentum conservation Eq. (2) as the most singular part of $V - P_{11}$:

$$U = V + \frac{\hbar^2}{4mT}\frac{\mathrm{d}^2\overline{V}}{\mathrm{d}x^2}. \tag{17}$$

As can be proved using Fourier transforms [1], the smooth effective potential is smoother by two degrees than the classical potential V; i.e., if V has a discontinuity, then U is once differentiable.

The double integration (over both space and temperature) provides sufficient smoothing so that the P_{11} term in the smooth effective potential cancels the leading singularity in the classical potential at a barrier (see Fig. 3), leaving a residual smooth effective potential with a lower potential height in the barrier region. This cancellation and smoothing makes the barriers partially transparent to the particle flow and provides the mechanism for particle tunneling in the QHD model. Note that the effective barrier height approaches zero as $T \to 0$. This effect explains in fluid dynamical terms why particle tunneling is enhanced at low temperatures. As $T \to \infty$, the effective potential approaches the classical double barrier potential and quantum effects in the QHD model are suppressed.

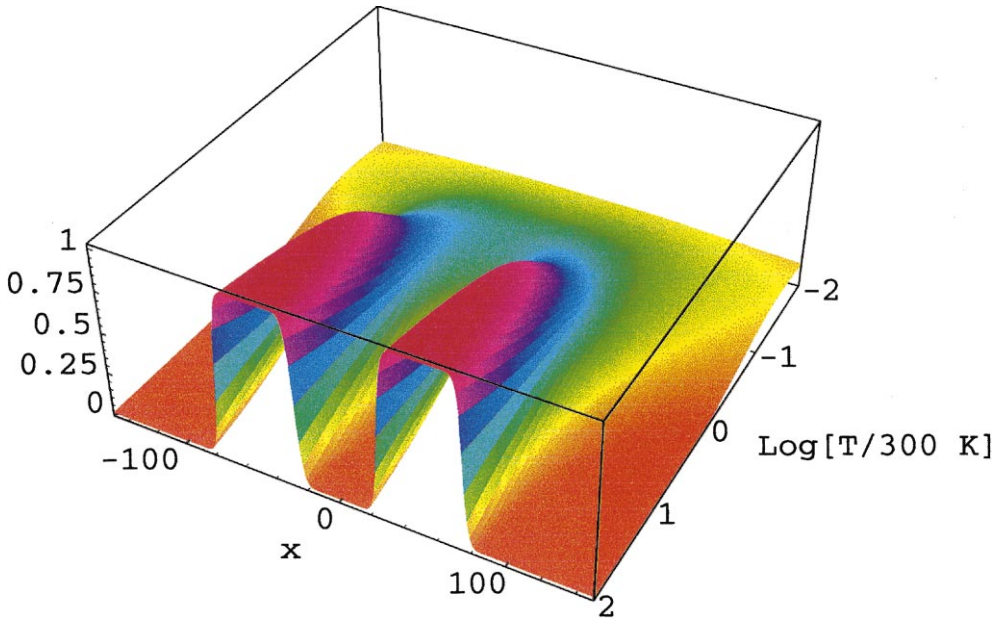

Fig. 3. Smooth effective potential for electrons in GaAs for 50 Å wide unit potential double barriers and 50 Å wide well as a function of x and $\log_{10}(T/300\ \mathrm{K})$.

Jump relations may be derived by integrating the QHD equations (1)–(3) across a wave:

$$-\frac{\hbar^2}{4mT}\left[\frac{\mathrm{d}^2\overline{V}}{\mathrm{d}x^2}\right] = [V], \tag{18}$$

$$\kappa\left[\frac{\mathrm{d}T}{\mathrm{d}x}\right] = -\frac{1}{2}nu[V], \tag{19}$$

where u is the normal velocity and $[\chi] = \chi_+ - \chi_-$ is the jump in χ across the wave. Eq. (18) says that the jump in the classical potential V is cancelled by the jump in the quantum part of the stress tensor and Eq. (19) says that the jump in $\mathrm{d}T/\mathrm{d}x$ is controlled by the jump in V.

3. Numerical methods

The smooth QHD transport equations are a set of hyperbolic PDEs with a parabolic heat conduction term in the energy conservation equation. Hyperbolic methods from computational gas dynamics like the ENO, piecewise parabolic, and discontinuous Galerkin methods are well suited for simulating the transient smooth QHD model. Steady-state solutions may be obtained as the asymptotic large t limit.

Here we will use a simple, robust steady-state method that is an order of magnitude faster than the transient solvers in 1D. The 1D steady-state smooth QHD equations are discretized [5] using a conservative upwind method adapted from computational fluid dynamics. The discretized equations are then solved by a damped Newton method. The simple upwind method outlined below is somewhat too dissipative for resolving shock waves sharply, and instead a higher order Godunov method should be used if the electron flow is transonic – see Refs. [11,12].

Well-posed boundary conditions for the 2D (and by extension 3D) classical hydrodynamic model are formulated in Ref. [13], assuming subsonic flow at the inflow and outflow boundaries. We note that in one dimension the smooth QHD model (with heat conduction) has two hyperbolic modes, one parabolic mode, and one elliptic mode. Thus, six boundary conditions are necessary for subsonic inflow and outflow. Well-posed boundary conditions for the resonant tunneling diode are $n = N$, and $T = T_0$ (or alternatively $\partial T/\partial x = 0$) at $x_{\min}$ and $x_{\max}$, with a bias ΔV across the device: $V(x_{\min}) = T\ \log(n/n_i)$ and $V(x_{\max}) = T\ \log(n/n_i) + e\Delta V$, where n_i is the intrinsic electron concentration.

Since the upwind method requires velocity values $u_{-1/2}, u_{1/2}, u_{3/2}, \ldots, u_{N-1/2}, u_{N+1/2}$ at the midpoints of the elements $l_i (i = 1, \ldots, N)$ connecting grid points $i-1$ and i, we use a staggered grid for u. Defining the velocities at midpoints of elements also resolves waves more sharply by avoiding the averaging of velocities defined at grid points i, $i \pm 1$ to obtain $u_{i-1/2}$ and $u_{i+1/2}$. The variables n, T, and V are defined at the grid points $i = 0, 1, \ldots, N-1, N$. The boundary conditions specify n, T, and V at $i = 0$ and $i = N$.

In 1D, the steady-state QHD model consists of the three nonlinear conservation laws for electron number, momentum, and energy, plus Poisson's equation:

$$\begin{bmatrix} f_n \\ f_u \\ f_T \\ f_V \end{bmatrix} = \frac{\mathrm{d}}{\mathrm{d}x}\begin{bmatrix} ug_n \\ ug_u \\ ug_T \\ 0 \end{bmatrix} + \begin{bmatrix} 0 \\ h_u \\ h_T \\ h_V \end{bmatrix} + \begin{bmatrix} 0 \\ s_u \\ s_T \\ s_V \end{bmatrix} = 0, \tag{20}$$

where

$$g_n = n, \tag{21}$$

$$g_u = mnu, \tag{22}$$

$$g_T = \frac{5}{2}nT + \frac{1}{2}mnu^2 + \frac{\hbar^2 n}{8mT}\frac{\mathrm{d}^2\overline{V}}{\mathrm{d}x^2} + nU, \tag{23}$$

$$h_u = \frac{\mathrm{d}}{\mathrm{d}x}(nT) + \frac{\mathrm{d}}{\mathrm{d}x}(nU) - V\frac{\mathrm{d}n}{\mathrm{d}x}, \tag{24}$$

$$h_T = -\frac{\mathrm{d}}{\mathrm{d}x}\left(\kappa\frac{\mathrm{d}T}{\mathrm{d}x}\right), \tag{25}$$

$$h_V = \epsilon\frac{\mathrm{d}^2 V_P}{\mathrm{d}x^2}, \tag{26}$$

$$s_u = \frac{mnu}{\tau_p}, \tag{27}$$

$$s_T = \left(\frac{3}{2}nT + \frac{1}{2}mnu^2 + \frac{\hbar^2 n}{8mT}\frac{\mathrm{d}^2\overline{V}}{\mathrm{d}x^2} - \frac{3}{2}nT_0\right)\Big/\tau_w, \tag{28}$$

$$s_V = e^2(N-n). \tag{29}$$

Note that wherever possible we difference the smooth effective potential U rather than V or $(\hbar^2/4mT)\ \mathrm{d}^2\overline{V}/\mathrm{d}x^2$ separately.

Equations $f_n = 0$, $f_T = 0$, and $f_V = 0$ are enforced at the interior grid points $i = 1,\ldots,N-1$, while equation $f_u = 0$ is enforced at the midpoints of the elements $l_i, i = 1,\ldots,N$.

In the conservative upwind method, the advection terms $\mathrm{d}(ug)/\mathrm{d}x$ in Eq. (20) are discretized using upwind differences:

$$\frac{\mathrm{d}}{\mathrm{d}x}(ug)_i \approx (u_{i+1/2}g_R - u_{i-1/2}g_L)/\Delta x, \tag{30}$$

where

$$g_{\mathrm{R}} = \begin{cases} g_i & (u_{i+1/2} > 0), \\ g_{i+1} & (u_{i+1/2} < 0), \end{cases} \qquad g_{\mathrm{L}} = \begin{cases} g_{i-1} & (u_{i-1/2} > 0), \\ g_i & (u_{i-1/2} < 0), \end{cases} \tag{31}$$

and second-order central differences are used for h_u, h_T, h_V, and s_T.

To linearize the discretized version of Eqs. (20), we use Newton's method:

$$J\begin{bmatrix}\delta n\\ \delta u\\ \delta T\\ \delta V\end{bmatrix} = -\begin{bmatrix}f_n\\ f_u\\ f_T\\ f_V\end{bmatrix} = -f, \quad \begin{bmatrix}n\\ u\\ T\\ V\end{bmatrix} \leftarrow \begin{bmatrix}n\\ u\\ T\\ V\end{bmatrix} + t\begin{bmatrix}\delta n\\ \delta u\\ \delta T\\ \delta V\end{bmatrix}, \tag{32}$$

where J is the Jacobian and t is a damping factor [14] between 0 and 1, chosen to insure that the norm of the residual f decreases monotonically.

There are two contributions to the quantum potential $\overline{V}$: the double barrier potential and the "self-consistent" electric potential from Poisson's equation. Note that second derivatives of $\overline{V}$ appear in the stress tensor and energy density, which then are differenced in the smooth QHD transport equations. Thus, we compute

$$\overline{V}'' = \overline{V}''_{\mathrm{B}} + \overline{V}''_{\mathrm{P}}. \tag{33}$$

$\overline{V}''_{\mathrm{B}}$ is just computed once since it only depends on the barriers and not on the applied voltage or state variables (n, u,T, V_{P}). In computing $\overline{V}''_{\mathrm{P}}$, we first use Poisson's equation to obtain

$$\overline{V}_{\mathrm{P}''}(\beta,x) = \frac{e^2}{\epsilon}\int_0^\beta \frac{\mathrm{d}\beta'}{\beta}\left(\frac{\beta'}{\beta}\right)^2\int \mathrm{d}x'\left(\frac{2m\beta}{\pi(\beta-\beta')(\beta+\beta')\hbar^2}\right)^{3/2} \times \exp\left\{-\frac{2m\beta}{(\beta-\beta')(\beta+\beta')\hbar^2}x'^2\right\}(N(x'+x)-n(x'+x)). \tag{34}$$

The convolution (34) can be computed efficiently using discrete Fourier transform algorithms.

4. Simulation of the RTD

We present simulations of a GaAs resonant tunneling diode with $Al_xGa_{1-x}As$ double barriers at 300 K. The barrier height is set equal to 0.1 eV. The diode consists of n^+ source (at the left) and drain (at the right) regions with the doping density $N = 10^{18}$ cm^{-3}, and an n channel with $N = 5 \times 10^{15}$ cm^{-3}. The channel is 200 Å long, the barriers are 25 Å wide, and the quantum well between the barriers is 50 Å wide. Note that the device has 50 Å spacers between the barriers and the contacts. We have chosen parameters to highlight differences between the original and smooth QHD models.

Fig. 4 illustrates the smooth effective potentials U_B (for the barriers), U_P (the Poisson contribution), and U (barrier plus Poisson contributions) for the resonant tunneling diode at 300 K at the voltage $\Delta V = 0.056$, where the current–voltage (I–V) curve peaks in Fig. 5.

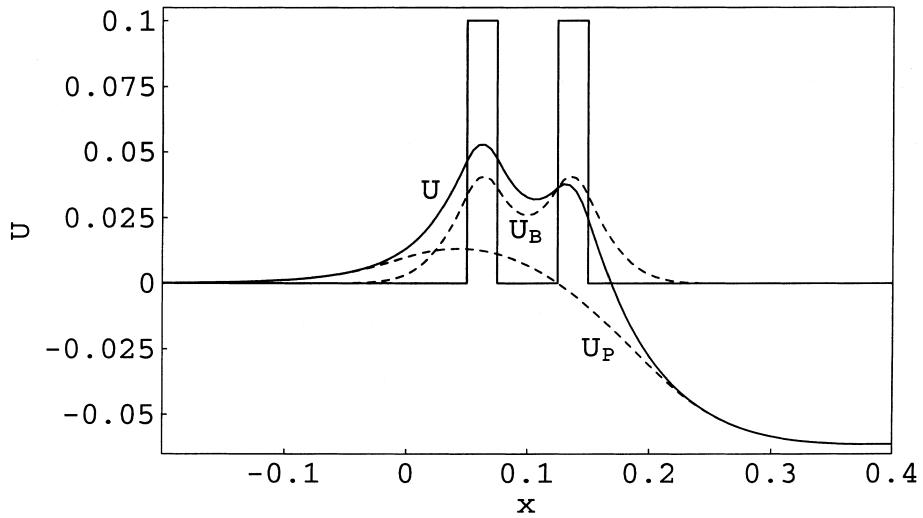

Fig. 4. Smooth effective potentials U, U_B, and U_P for an applied voltage of 0.056 V for 0.1 eV double barriers at 300 K. x is in 0.1 microns.

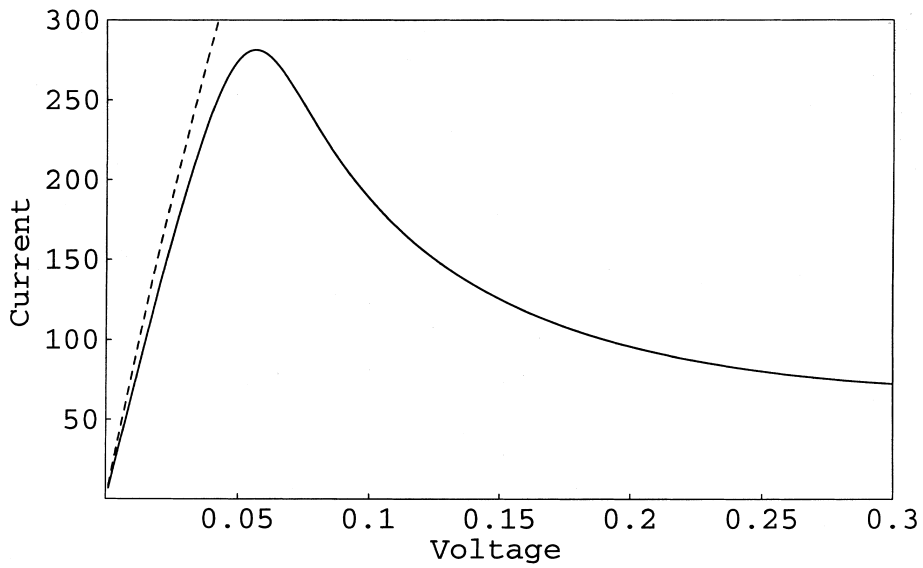

Fig. 5. Current density in kiloamps/cm^2 verses voltage for the resonant tunneling diode at 300 K. The solid curve is the smooth QHD computation and the dotted line is the $O(\hbar^2/(mTl^2))$ computation. The barrier height is 0.1 eV.

Smooth QHD simulations of the resonant tunneling diode exhibit enhanced negative differential resistance when compared to simulations using the original $O(\hbar^2/(mTl^2))$ QHD model. The current–voltage curve for the resonant tunneling diode at 300 K is plotted in Fig 5. It is interesting that the original $O(\hbar^2/(mTl^2))$ QHD model predicts very different I–V curves – in fact, the original $O(\hbar^2/(mTl^2))$ QHD model fails to produce negative differential resistance for this device.

Note that the I–V curves agree in the thermal equilibrium limit $V \to 0$. Thus, we believe the original $O(\hbar^2/(mTl^2))$ QHD model is only valid for applied voltages ΔV for which $\beta\Delta V \ll 1$.

5. Conclusion

In his lectures on *Statistical Mechanics* [15], Feynman derives an effective quantum potential by a Gaussian smoothing of the classical potential. After demonstrating that the effective free energy based on the effective potential is accurate for smooth classical potentials like the anharmonic oscillator, he goes on to say that "it fails in its present form when the classical potential has a very large derivative as in the case of hard-sphere interatomic potential" – or for potential barriers in quantum semiconductor devices. In this investigation, we have discussed an extension of Feynman's ideas to a smooth effective potential for the quantum hydrodynamic model that is valid for the technologically important case of potentials with discontinuities.

Simulations of the resonant tunneling diode using the Wigner–Boltzmann/Poisson equations are in progress to demonstrate that the smooth QHD model gives better agreement with the more complete quantum kinetics than the $O(\hbar^2/(mTl^2))$ model. We will also map out the parameter range over which the smooth QHD solutions (first three moments) accurately reflect the solutions to the full Wigner–Boltzmann equation. There should be a technologically important range of parameters (device size, ambient temperature, potential barrier height, applied voltage, semiconductor material, etc.) in which the smooth QHD model gives solutions and I–V curves that are very close to those given by the Wigner–Boltzmann/Poisson system.

References

[1] C.L. Gardner, C. Ringhofer, Smooth quantum potential for the hydrodynamic model, Physical Review E 53 (1996) 157–167.
[2] C.L. Gardner, C. Ringhofer, Approximation of thermal equilibrium for quantum gases with discontinuous potentials and application to semiconductor devices, SIAM Journal on Applied Mathematics 58 (1998) 780–805.
[3] G.B. Whitham, Linear and Nonlinear Waves, Wiley, New York, 1974.
[4] H.L. Grubin, J.P. Kreskovsky, Quantum moment balance equations and resonant tunnelling structures, Solid-State Electronics 32 (1989) 1071–1075.
[5] C.L. Gardner, The quantum hydrodynamic model for semiconductor devices, SIAM Journal on Applied Mathematics 54 (1994) 409–427.
[6] C.L. Gardner, Resonant tunneling in the quantum hydrodynamic model, VLSI Design 3 (1995) 201–210.
[7] Z. Chen, B. Cockburn, C.L. Gardner, J.W. Jerome, Quantum hydrodynamic simulation of hysteresis in the resonant tunneling diode, Journal of Computational Physics 117 (1995) 274–280.
[8] P. Pietra, C. Pohl, Weak limits of the quantum hydrodynamic model, VLSI Design to appear.
[9] C.L. Gardner, Hydrodynamic and Monte Carlo simulation of an electron shock wave in a one micrometer $n^+ - n - n^+$ diode, IEEE Transactions on Electron Devices 40 (1993) 455–457.
[10] H.L. Grubin, T.R. Govindan, J.P. Kreskovsky, M.A. Stroscio, Transport via the Liouville equation and moments of quantum distribution functions, Solid-State Electronics 36 (1993) 1697–1709.
[11] C.L. Gardner, J.W. Jerome, C.W. Shu, The ENO method for the hydrodynamic model for semiconductor devices, in: High Performance Computing, 1993: Grand Challenges in Computer Simulation, The Society for Computer Simulation, San Diego, 1993, pp. 96–101.
[12] E. Fatemi, C.L. Gardner, J.W. Jerome, S. Osher, D.J. Rose, Simulation of a steady-state electron shock wave in a submicron semiconductor device using high-order upwind methods, in: Computational Electronics: Semiconductor Transport and Device Simulation, Kluwer Academic Publishers, Boston, 1991, pp. 27–32.
[13] F. Odeh, E. Thomann, On the well-posedness of the two-dimensional hydrodynamic model for semiconductor devices, Compel 9 (1990) 45–47.
[14] R.E. Bank, D.J. Rose, Global approximate Newton methods, Numerische Mathematik 37 (1981) 279–295.
[15] R.P. Feynman, Statistical Mechanics: A Set of Lectures, Benjamin Reading, MA, 1972.